Neurocomputing 73 (2010) 784–794

Contents lists available at ScienceDirect

Neurocomputing

journal homepage: www.elsevier.com/locate/neucom

No-reference image quality assessment in contourlet domain

Wen Lu [a], Kai Zeng [a], Dacheng Tao [b,*], Yuan Yuan [c], Xinbo Gao [a]

[a] School of Electronic Engineering, Xidian University, Xi'an 710071, China
[b] School of Computer Engineering, Nanyang Technological University, 50 Nanyang, Avenue, 639798 Singapore, Singapore
[c] School of Engineering and Applied Science, Aston University, Birmingham B4 7ET, UK

ARTICLE INFO

Article history:
Received 3 June 2009
Received in revised form
18 October 2009
Accepted 18 October 2009
Communicated by T. Heskes
Available online 20 November 2009

Keywords:
Image quality assessment
No reference
Image modeling
Contourlets

ABSTRACT

The target of no-reference (NR) image quality assessment (IQA) is to establish a computational model to predict the visual quality of an image. The existing prominent method is based on natural scene statistics (NSS). It uses the joint and marginal distributions of wavelet coefficients for IQA. However, this method is only applicable to JPEG2000 compressed images. Since the wavelet transform fails to capture the directional information of images, an improved NSS model is established by contourlets. In this paper, the contourlet transform is utilized to NSS of images, and then the relationship of contourlet coefficients is represented by the joint distribution. The statistics of contourlet coefficients are applicable to indicate variation of image quality. In addition, an image-dependent threshold is adopted to reduce the effect of content to the statistical model. Finally, image quality can be evaluated by combining the extracted features in each subband nonlinearly. Our algorithm is trained and tested on the LIVE database II. Experimental results demonstrate that the proposed algorithm is superior to the conventional NSS model and can be applied to different distortions.

1. Introduction

Among most of the applications, the visual information in an image is ultimately received by human beings, it is intuitively reasonable to score the image quality subjectively [1]. However, subjective *image quality assessment* (IQA) methods are expensive and time consuming and so they cannot be easily and routinely performed for many scenarios, e.g., real time systems. The current alternative to subjective IQA is objective IQA [3], which tries to assign scores that are in meaningful agreement with subjective result. These results can be used to automatically assess the image quality.

Objective quality metrics can be divided into reference [6,8,26–29] and no-reference [9] methods, depending on whether the method utilizes reference information. Reference methods usually provide more precise assessments of image quality than non-reference methods. The objective measures used in reference methods include *peak signal-to-noise ratio* (PSNR), *structural similarity* (SSIM) [10] and the *visual information fidelity* (VIF) [11]. These methods are found to be highly correlated with subjective scores. However, their application is limited because the reference information may not be available or too expensive to be obtained in many scenarios [2,4].

NR methods output evaluation results without the reference information. Instead, they rely on strong hypotheses of one or a set of predefined distortions, e.g., the blocking effect in JPEG, the ringing and blurring artifacts in JPEG2000. Wang et al. [12] proposed an effective and efficient quality assessment model for JPEG images. Bovik and Liu [13] modeled the blocking-artifacts to measure the compressed image quality. Mei et al. [14] proposed a novel spatio-temporal quality assessment scheme by using low-level content features for home videos. Luo and Tang [15] evaluated visual quality by using high-level semantic features are utilized. Badu et al. [16] applied the edge amplitude and length, the background luminance, and activity to IQA. Sheikh et al. [9] proposed an NR IQA metric that uses natural scene statistics (NSS) for JPEG2000 compressed images.

The existing state-of-art approach employs the NSS model [9] to do IQA. This is based on the observation that natural images exhibit certain common statistical characteristics which can be represented by a mathematical model and disturbed by the distorted processing. For IQA, degree of distortion can be quantized by measuring the change of statistical characteristics model. Sheikh's NSS model metrics models the marginal distribution [17] and the joint statistics [18,19] of wavelet coefficients to evaluate JPEG2000 compressed natural images, which outperforms many other existing methods. However, the experimental results also show that this approach is only applicable to JPEG2000 compressed images. In other words, the method is only effective for the image which is processed based on wavelet

* Corresponding author.
E-mail address: dacheng.tao@gmail.com (D. Tao).

0925-2312/$ - see front matter © 2009 Elsevier B.V. All rights reserved.
doi:10.1016/j.neucom.2009.10.012

transform. Moreover, wavelet transforms fail to explicitly capture directional information which is necessary for image modeling. Therefore, there is still a big space to further improve the performance of NR IQA [5].

In this paper we propose to deal with the aforementioned problems by applying contourlets. The principle advantage of applying contourlet transform is that its characteristics can be used to model images that suffer from directional multiscale dependencies, which are sensitive to image degradation and therefore can be used to evaluate the quality without the corresponding reference images. The mutual information between contourlet coefficients at different spaces, scales and directions are first modeled by calculating the joint histogram of reference and predicted coefficients. Then, in order to eliminate the effect of image content, an image-dependent threshold is employed to divide the joint space as two regions. Finally, image quality can be predicted by pooling and mapping a signification region, which is most represented for distortion, to suitable measurement. Because the contours and smooth curves are dominant in image structure which is most sensitive for human eyes, modeling these features using contourlet transform is an effectual metrics for IQA [7].

The remainder of the paper is organized as follows. Section 2 introduces NR IQA framework of employing the image modeling in contourlet domain. In Section 3, experimental results are given. Finally, conclusion is showed in Section 4.

2. Image modeling for no-reference image quality assessment in contourlet domain

Based on the statement above, we develop an improved image model in contourlet domain to do image quality assessment, which quantifies the variation of the nonlinear dependencies between contourlet coefficients to measure the image degradation. Fig. 1 shows the framework of the proposed and it works with following stages: (1) contourlets [20] is utilized to achieve an optimal approximation rate of piecewise smooth functions, (2) the relationship of contourlet coefficients is represented by the joint statistics distribution, (3) the statistics of contourlet coefficients are applicable to indicate variation of image quality, (4) an image-dependent threshold is adopted to reduce the effect of content to the statistical model, and (5) image quality can be obtained by combining the extracted features in each subband nonlinearly.

2.1. A brief introduction of the contourlet

Contourlet is proposed by Do and Vetterli [20], which is also known as *pyramidal directional filter banks* (PDFBs), is an efficient representation for image geometry structure. It combines the multiscale and multidirection decomposition together, employs *Laplacian pyramid* (LP) to capture the point discontinuities and then uses *directional filter banks* (DFB) to link these point discontinuities into linear structures. Its characteristics, such as good spatial localization, good direction selectivity, anisotropy, can be utilized to construct a sparse expansion for typical images that are piecewise smooth away from smooth contours. Fig. 2 shows the framework of contourlet decomposition which applies the LP and DFB in succession to generate subbands with different spatial frequencies and directions. An example of the contourlet decomposition of the "caps" image is shown in Fig. 6(a).

2.2. Relationship of contourlet coefficients

Contourlet transform is introduced to decompose images and produce coefficients at different subbands, relationship of whose coefficients are reflected by the mutual information among scale, direction and adjacent. Distribution of these coefficients allows us utilize three fundamental factors to represent images, including scale, space and direction [21].

Fig. 3 illustrates the relationships among contourlet coefficients. For each contourlet coefficient *C*, it has eight adjacent *neighbors* (*NC*), one *parent* (*PC*) and one *grandparent* (*GC*) in the relevant coarser scale and several *cousins* (*CC*) in the same scale and spatial location but different directions. The dependency of *C* to its relative is shown in Fig. 3.

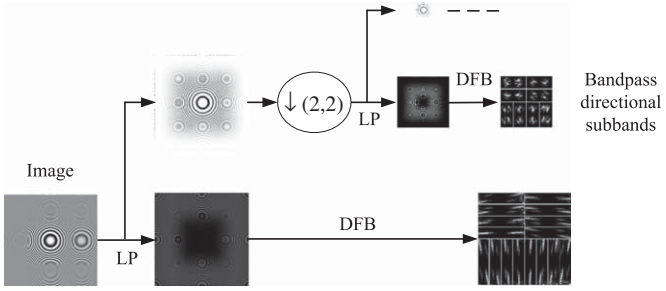

Fig. 2. The scatter plot of contourlet decomposition.

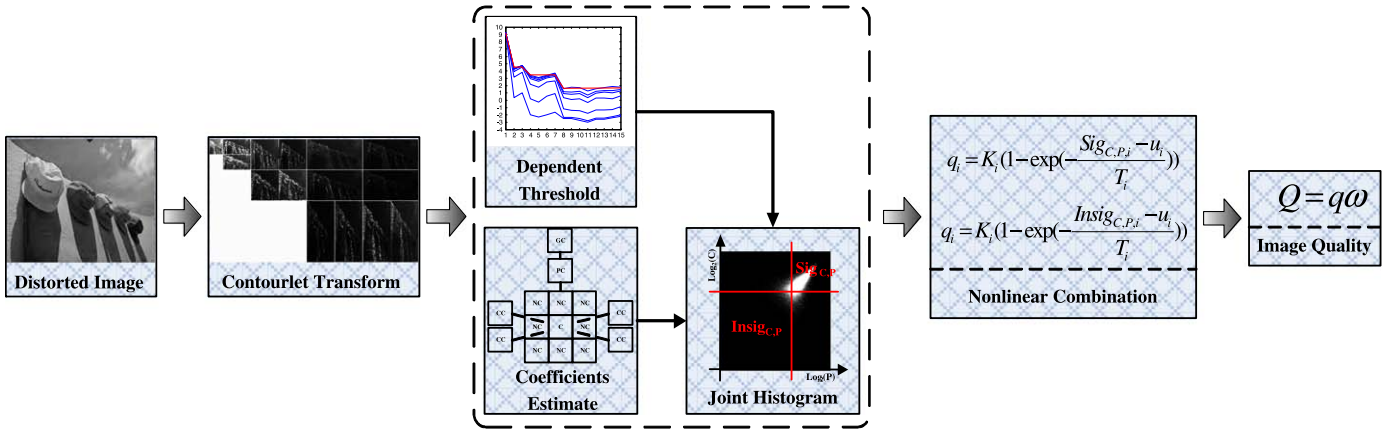

Fig. 1. Framework of the proposed NR IQA metrics, which utilizes image modeling in the contourlet domain to simulate the function of human eyes for measuring image perceptual quality.

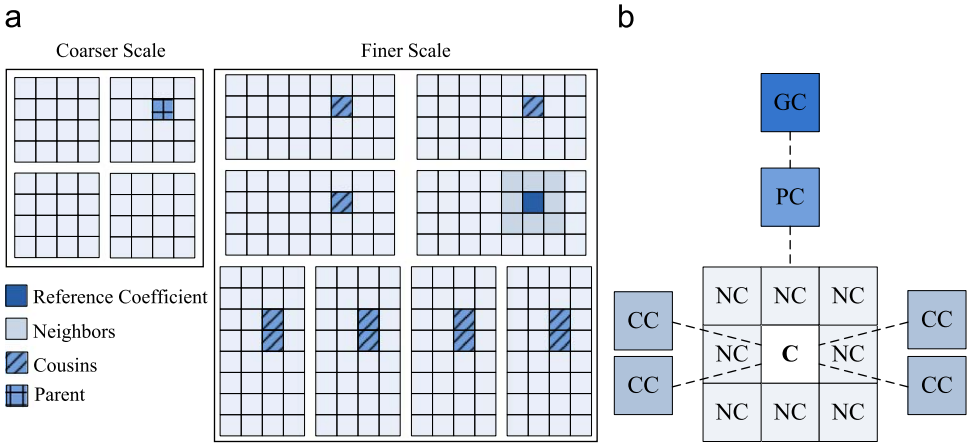

Fig. 3. Relationships of contourlet coefficients.

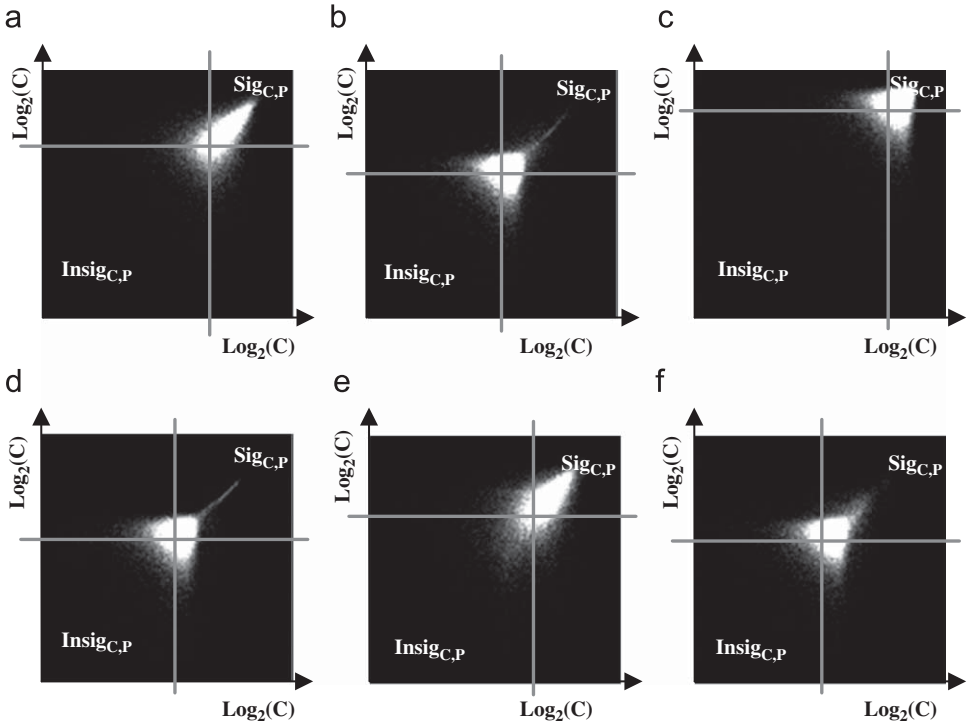

Fig. 4. Joint histograms of ($\log_2 P$, $\log_2 C$) for one subband of different distorted images: (a) Natural, (b) JPEG2000, (c) WN, (d) FF (e) JPEG and (f) Gblur.

Contourlet coefficient's magnitude is modeled by combining all correlation, conditioned on the magnitude of the linear prediction of the coefficient, P, as follows [9,19]:

$$C = MP + N \tag{1}$$

$$P = \sum_{i=1}^{n} l_i C_i \tag{2}$$

where M and N are assumed to be independent zero-mean random variables, the coefficients C_i come from an n coefficient neighborhood of C in space, scale, and orientation, and l_i are linear prediction parameters.

Therefore, based on the dependencies between contourlet coefficients, the mutual information of C and P predicted by (2) can be modeled by constructing their joint histograms as shown in Section 2.3.

2.3. Statistics of distorted natural images

Because the statistical model stated above is stable across different natural images, different distortions could disorder this kind of regularity in different ways. The scale, direction, and space dependency of C and P can be described by the logarithmic joint histogram of them.

For natural images, the C and P have strong nonlinear dependence on logarithmic axes, as illustrated in Fig. 4(a). Fig. 4 shows the joint histograms of ($\log_2 P$, $\log_2 C$) for one natural image subband and its correspondence five distorted version which will

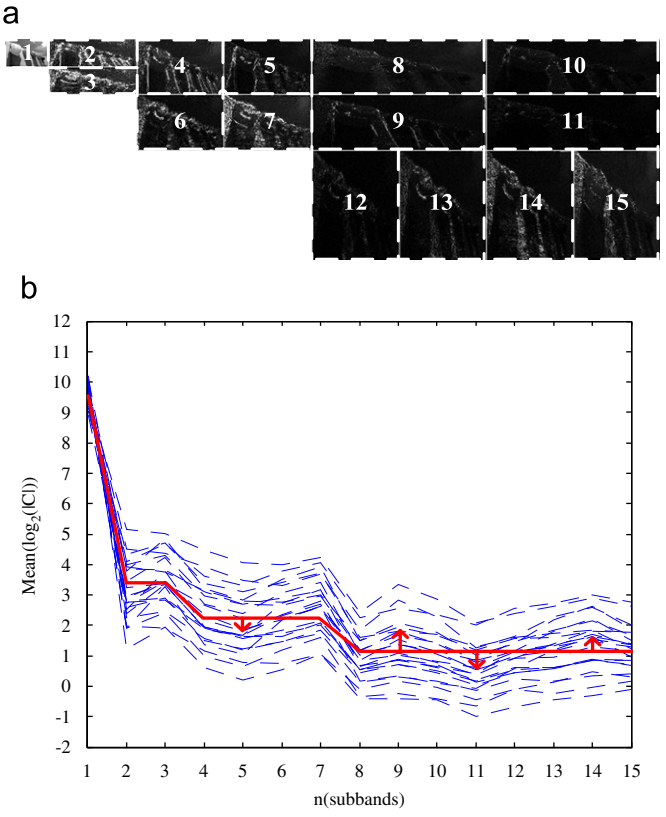

Fig. 5. *Mean*($\log_2(|C|)$) versus subband enumeration index. (a) The subband serial number used in (b) and Fig. 8(b) *Mean*($\log_2(|C|)$) falls off with the decrease of scale.

be explained in Section 3.1. It is obvious that the shape of joint histogram is affected by contamination. Then, an image-dependent threshold, which will be introduced in Section 2.4, is applied to divide the joint histogram plane into four parts. And define the image features as follow:

$$Sig_{C,P} = \frac{n_{C>T,P>T}}{n_{C,P}} \tag{3}$$

$$Insig_{C,P} = \frac{n_{C<T,P<T}}{n_{C,P}} \tag{4}$$

where $n_{C>T,P>T}$ and $n_{C<T,P<T}$ is the number of significant and insignificant C and P in subband, $n_{C,P}$ is the total number of contourlet coefficient in subband, T is image dependent threshold.

2.4. Image-dependent threshold

One significant characteristic of image model is that some attributes of the model should be stable, regardless of the variation of image content. But the distribution of joint histogram presented in Section 2.3 changes not only with the distortion of image, but also varies with the image content. So, we need an image-dependent threshold to decide the proportion of $Sig_{C,P}$ and $Insig_{C,P}$. Considering the complexity and precise, *Mean*($\log_2(|C|)$) of subband is employed as threshold to extract the necessary proponent.

Fig. 5 shows the *Mean*($\log_2(|C|)$) versus subband enumeration index. Fig. 5(a) illustrates the subband serial number n used in (b). Fig. 5(b) depicts the *Mean*($\log_2(|C|)$) for natural images and corresponding fit polygonal line (solid red line). From this result, we can observe that logarithmic magnitude of the

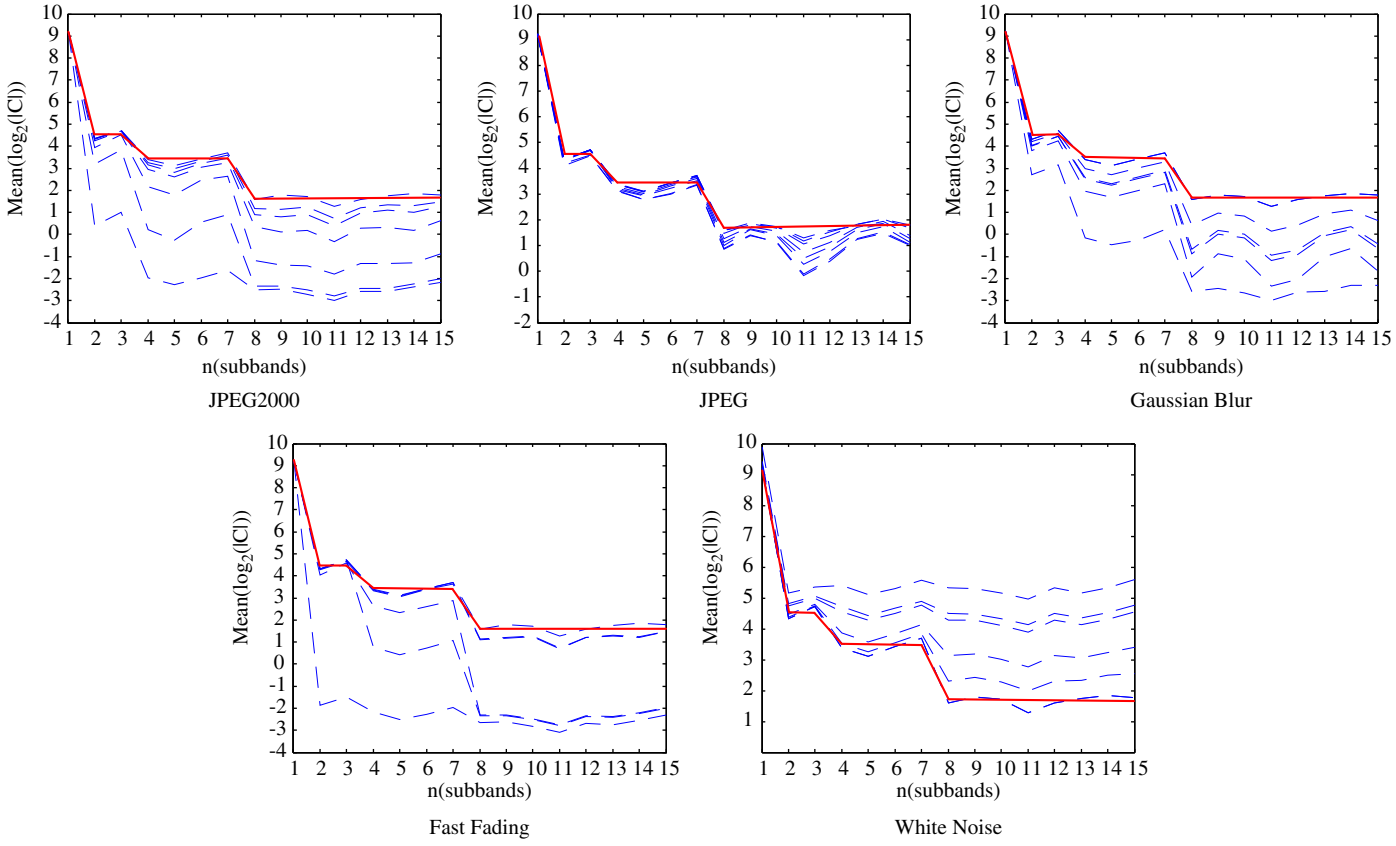

Fig. 6. *Mean*($\log_2(|C|)$) versus subband enumeration index for natural image and their different distorted versions.

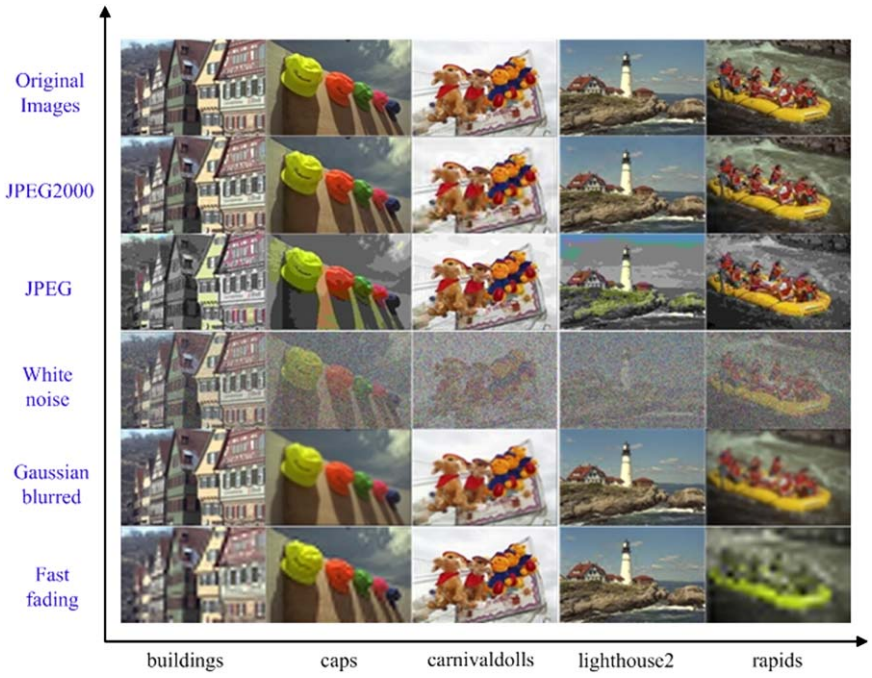

Fig. 7. Sample images and their respective distorted images (from top to bottom: original images, JPEG2000 compress, JPEG, White noise, Gaussian blurred, Fast fading).

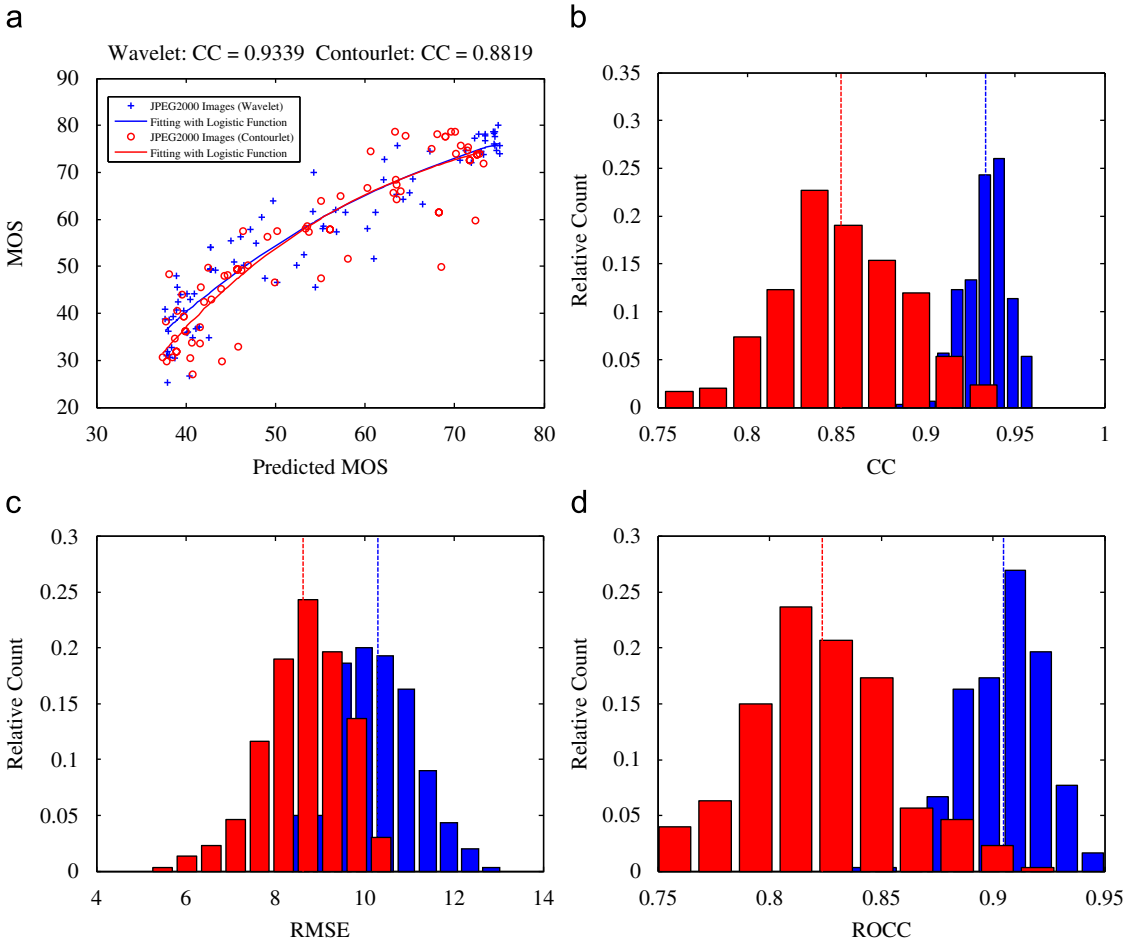

Fig. 8. The comparison of the proposed and paper [9] on JPEG2000.

contourlet coefficients inside the same scale changes approximate regularly due to the DFB decomposition. On the other hand, since the LP transform decompose image into different scales, the logarithmic mean of contourlet coefficients show the biggest difference between each scale, and its difference is relatively robust to changes in the image content.

Fig. 6 depicts the $Mean(\log_2(|C|))$ for an image with different types and degrees of distortion and the corresponding fits (solid red line). From Fig. 6, we can see that the $Mean(\log_2(|C|))$ of images with different distortions has different degrees of deviation from that of natural image. For JPEG2000, JPEG, Gblur and FF images, $Mean(\log_2(|C|))$ changes approximately in the same way, that is the worse of image quality, the closer of $Mean(\log_2(|C|))$ towards zero. But white noisy images have the opposite property, $Mean(\log_2(|C|))$ tends to far from zero as the quality of images become worse. Because white noise tends to increase the texture of image, which can be regarded as another form of contour, and other types of distortion try to smooth the edges in image.

Another extremely significant observation from Fig. 6 is that for all those types of distortion, the degradation of image reflects on almost all subbands in contourlet domain. But in wavelet domain, only partial subbands are obviously affected by distortion [9]. So, we could employ the statistical modeling in contourlet domain more precisely than those of wavelet to evaluate the image visual quality.

We train different parameters between each scale by the natural images in the training set. In some subbands, in order to compensate the deviation of mean value of contourlet coefficients from the $Mean(\log_2(|C|))$, we specify the offset parameters to calculate the threshold more precisely. Thus, we use above observation to calculate the image dependent thresholds as follows:

$$T_{scale,i} = C_l + diff_{i,l} \tag{5}$$

$$T_{subband,j} = T_{scale,i} + T_{offset,i,j} \tag{6}$$

where C_l is the $Mean(\log_2(|C|))$ of coarsest subband, $T_{scale,i}$ is the JND threshold of i-th scale, $diff_{i,l}$ is the difference of $Mean(\log_2(|C|))$ between i-th scale and the coarsest, $T_{subband,j}$ is the JND threshold of j-th subband in i-th scale, $T_{offset,i,j}$ is the offset of j-th subband in i-th scale. Both $diff_{i,l}$ and $T_{offset,i,j}$ can be learned by numerical minimization that attempts to minimize the error in the quality predictions over the training set. In this way, through the adjustment of threshold, our algorithm becomes more robust to changes in the image content.

Table 1
The comparison of two algorithms on JPEG2000.

	CC	RMSE	ROCC
Ref. [9]			
Mean	0.9332	10.2955	0.9047
St. D.	0.0127	0.8633	0.0185
Proposed			
Mean	0.8527	8.6205	0.8238
St. D.	0.0351	0.9209	0.0324

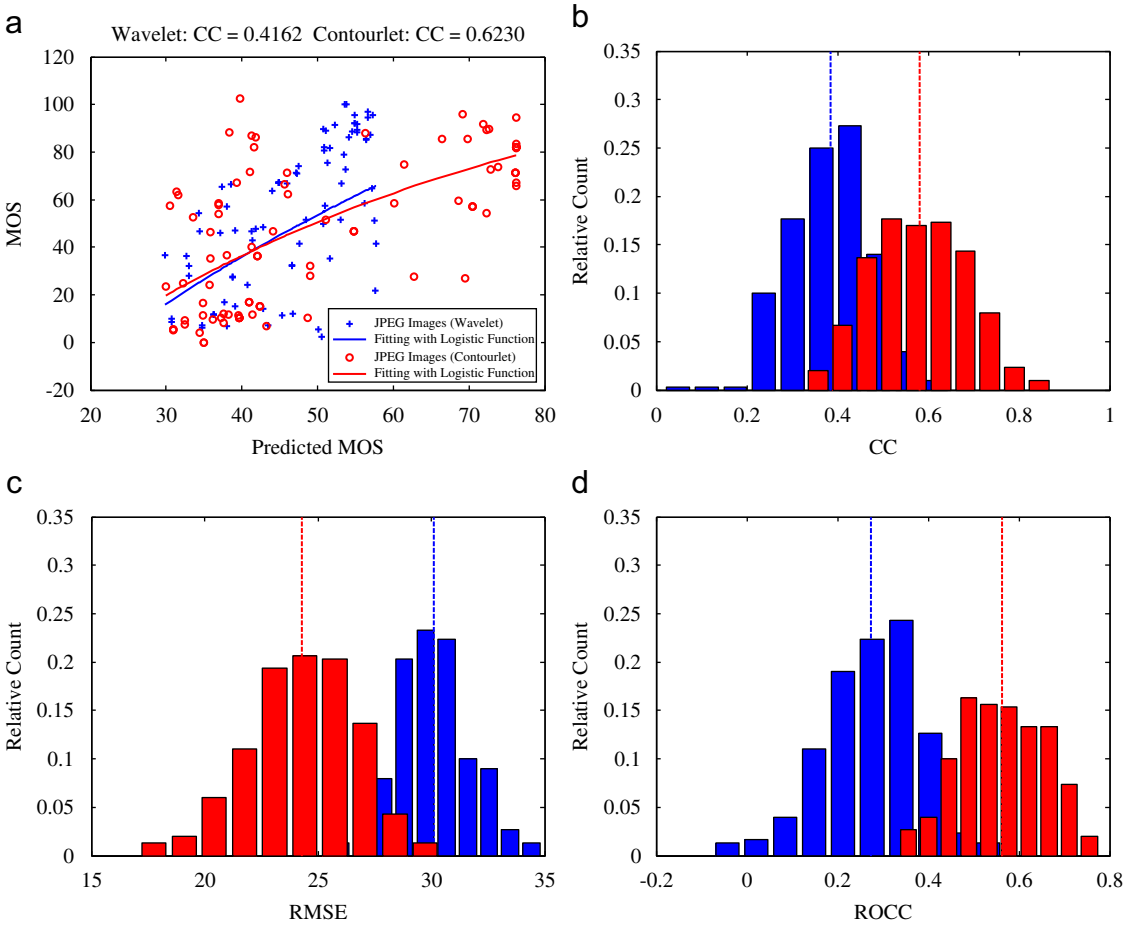

Fig. 9. The comparison of the proposed and [9] on JPEG.

2.5. Calculation of image quality

Because the dependency of C and P is varied with the different types of distortion, the distribution of joint histogram could be an indicator for the unnaturalness and visual quality. From Figs. 4 and 6, we could observe that the distortion scheme, like JPEG2000, FF, JPEG and Gblur, would push the joint histogram toward zero, while white noise would add extra information on high frequency so that more C and P would be regard as significant. Therefore, we choose $Insig_{C,P}$ as the quality indicator of WN images and choose $Sig_{C,P}$ for other distorted images.

Since the distortion is different in each scale and direction, a nonlinear combination is utilized to integrate these features to obtain the final image quality. Therefore, a nonlinear transform of these features is employed firstly to calculate the quality of each subband as follows:

$$q_i = K_i\left(1\text{-}\exp\left(\frac{(Sig_{C,P,i}|Insig_{C,P,i})\text{-}u_i}{T_i}\right)\right) \tag{7}$$

Table 2
The comparison of two algorithms on JPEG.

	CC	RMSE	ROCC
Ref. [9]			
Mean	0.3837	30.1172	0.2732
St. D.	0.0872	1.5913	0.1055
Proposed			
Mean	0.5810	24.3001	0.5623
St. D.	0.1055	2.3811	0.0952

where q_i is the predicted image quality, $Sig_{C,P,i}$ or $Insig_{C,P,i}$ is probability of significant or insignificant C and P for the i-th subband, K_i, u_i and T_i are the fitting parameters for the i-th subband that can be trained from the training set.

Finally, we weighted each predicted image quality to calculate the final quality of whole image.

$$q = [q_1, q_2, q_3, \ldots, q_n]$$

$$Q = q\omega \tag{8}$$

where the weights ω are learned by optimizing the predicted precision upon the training set.

3. Experimental results

3.1. Simulation details

We validate our algorithm on the *laboratory for image & video engineering* (LIVE) database [22]. This database contains 29 high-resolution 24 bits/pixel RGB color images as reference and corresponding five types of distorted images: 175 JPEG, 169 JPEG2000, 145 *White Noisy* (WN), 145 *Gaussian blurred* (Gblur) and 145 *Fast-Fading* (FF) Rayleigh channel noisy images at a range of quality levels (the sample images are shown in Fig. 7). The *difference mean opinion scores* (DMOS) of the image is provided to describe the subjective quality of the degraded image.

In order to train and test, the database is divided into two subsets. The training database consists of 15 natural images and their corresponding distorted version. The other 14 images and

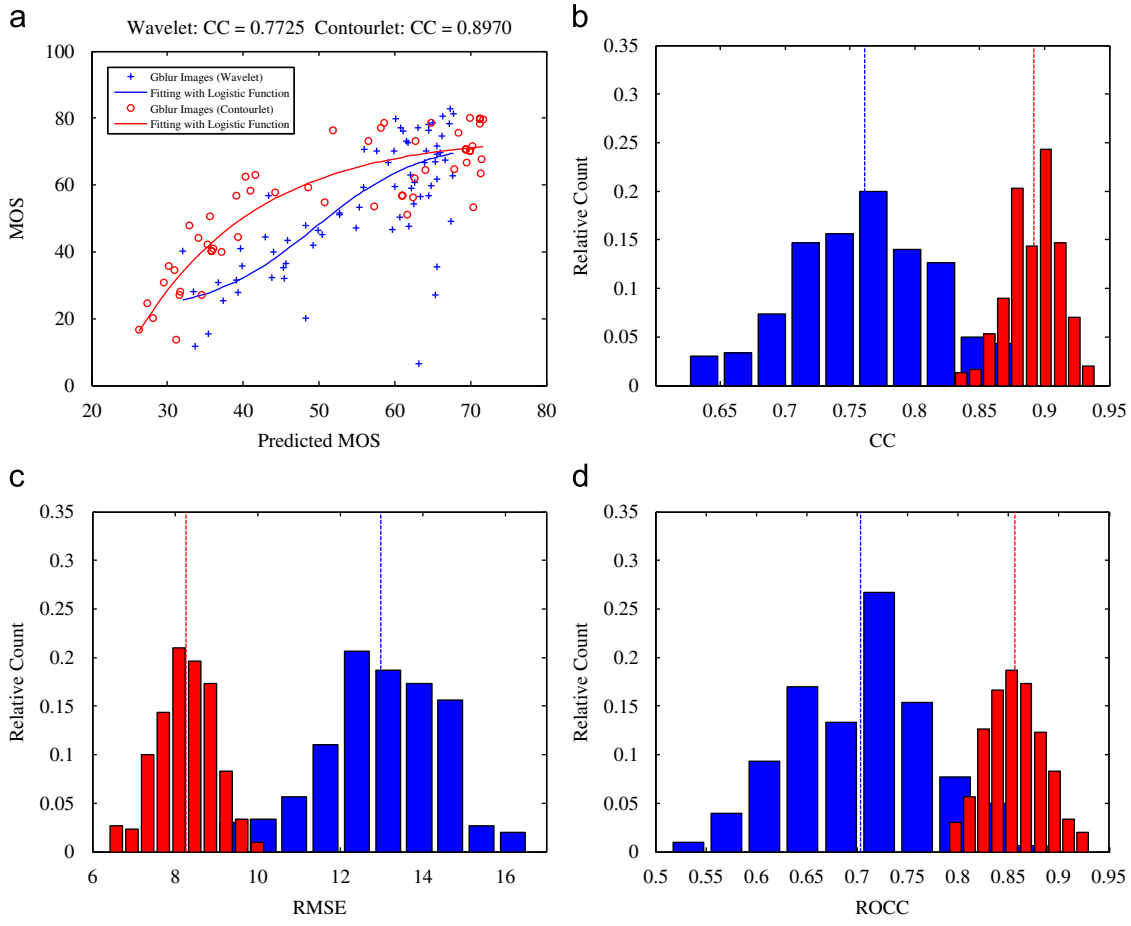

Fig. 10. The comparison of the proposed and [9] on Gblur.

their distorted version are used for testing. There is no overlap between these two groups and all natural images are selected randomly.

The luminance component of images normalized to be a *root-mean-squared* (RMS) value of 1.0 per pixel has been employed to validate our algorithm. The biorthogonal 9/7 filter with three levels of decomposition is used for *Laplacian Pyramid* (LP) and the ladder filter known as "*pkva*" is employed for *Directional Filter Bank* (DFB). The difference between each scale for estimating the subband coefficient is learned from the uncompressed images in the training set. The weights ω are learned using nonnegatively constrained least-squares fit over the training data (MATLAB command *lsqnonneg*). The minimization over the threshold offsets, as well as for the fitting parameters, is done by unconstrained nonlinear minimization (MATLAB command *fminsearch*).

Table 3
The comparison of two algorithms on Gblur.

	CC	RMSE	ROCC
Ref. [9]			
Mean	0.7611	12.9854	0.7033
St. D.	0.0545	1.4523	0.0689
Proposed			
Mean	0.8917	8.2741	0.8561
St. D.	0.0203	0.7004	0.0283

3.2. Quality calibration

Since it is allowed to make a nonlinear mapping between subjective and objective scores in application, the variance-weighted regression analysis provided by *Video Quality Expert Group* (VQEG) [23] is employed, while the fitting was done by weighted least squares function (Matlab command: *nlinfit* and *nlpredic*):

$$Quality(x) = \omega\left[\frac{\beta_1\text{-}\beta_2}{1+\exp(\text{-}(x\text{-}\beta_3)/\beta_4)} + \beta_2\right] \tag{9}$$

where ω is the reciprocal of the variance of subjective scores, β_i $(i=1,2,3,4)$ are the fitting parameters. The initial values are given in [23].

3.3. Results

The proposed needs train the parameters on the training set firstly and validate it on the testing set. Because the parameters are different when computed from the different training sets, the experimental results obtained are also different, it is inconvincible to demonstrate the performance of algorithm by only run one time. Thus, we employ three objective criterions for evaluation after several run of algorithm, including Pearson linear *correlation coefficient* (CC), *root mean square error* (RMSE) and *Spearman rank order correlation coefficient* (ROCC).

3.3.1. Results of JPEG2000 images

Fig. 8 shows the comparison of the proposed and [9] on JPEG2000 images, Table 1 gives the prediction of the algorithm on

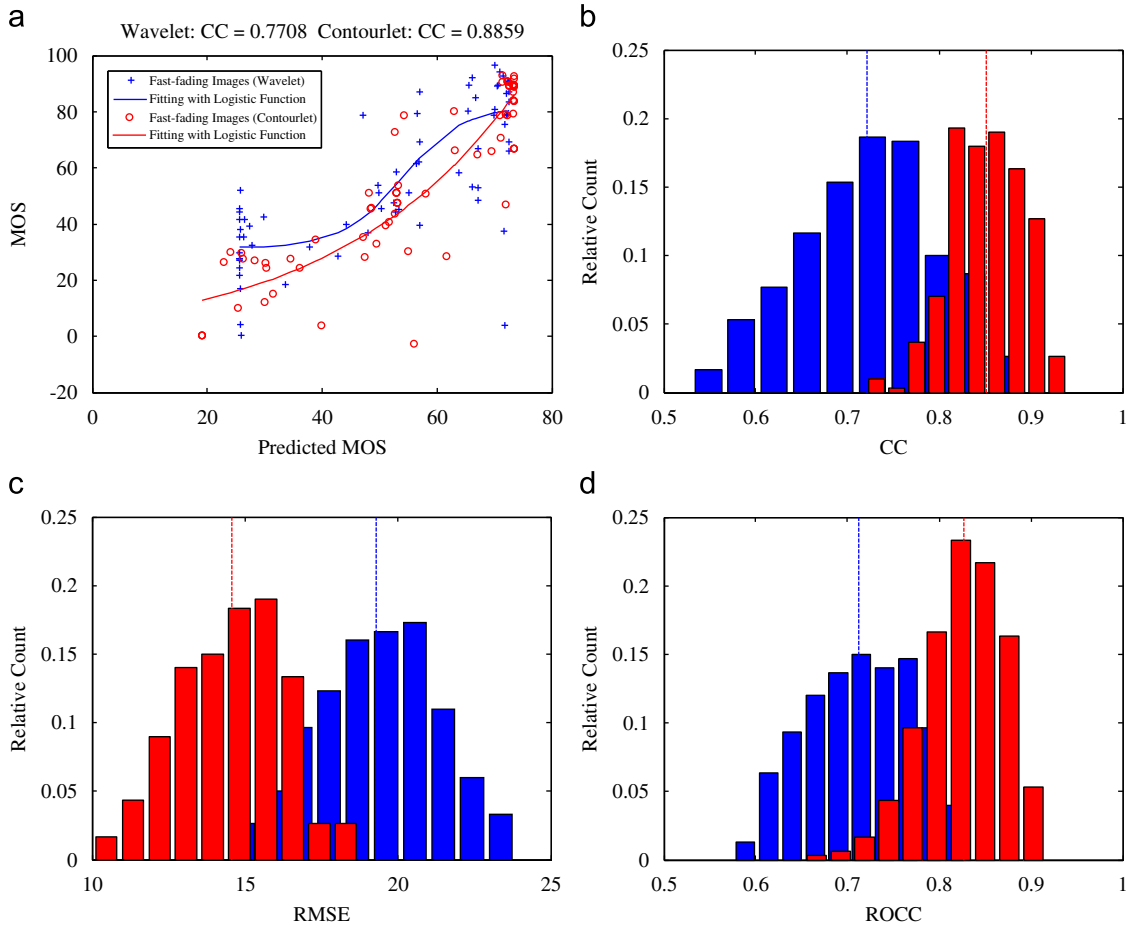

Fig. 11. The comparison of the proposed and paper [9] on FF.

the testing data for one of the runs against the MOS, and (b)–(d) illustrate the normalized histograms of CC, RMSE and ROCC for several runs, with red bars for the proposed method and blue for [9]. The dashed lines show the mean value. The mean and *standard deviation* (St. D.) of each criterion are compared.

For comparison, [24] proposed an NR perceptual blur metric with CC of 0.85 on the same database. In [9], since the blur and ringing artifact of JPEG2000 root from wavelet transform, it is more suitable to model image in wavelet domain. However, the algorithm proposed in [9] only takes effect to JPEG2000 images. When it comes to other types of distortion, the contourlet statistics model outperforms it.

3.3.2. Results of JPEG images

The comparison of the proposed and [9] on JPEG images are shown in Fig. 9. The meaning of (a)–(d) is the same as that in Fig. 8. The statistical comparison of each criterion is given in Table 2. We can see that the proposed has get better results than the method in [9]. Because the predominant distortion of JPEG image is the blocking artifact which induced by block-based DCT transform, frequency proponents do not effected obviously with the change of distortion. In addition, contourlets is good at capturing the smooth contour, and not sensitive to the block structure.

3.3.3. Results of Gblur images

Because the artifacts of Gblur images include not only the changes of luminance and texture, but also the shift and drop of phase, the high frequency of images have been influenced by distortion. The scatter diagram and performance index of the proposed and [9] method for those three criterions to Gblur images are shown in Fig. 10. Table 3 presents the statistical results.

We can see that, the proposed algorithm could capture the change of frequency proponents, and quantize this degradation effectively, which can be used to measure the perceptual quality of images.

3.3.4. Results of FF images

Fast-fading images are composed by distorted images which are degraded by bit errors during transmission of compressed JPEG2000 bit-stream over a simulated wireless channel. Besides the blur and ringing effect, distortion mainly conclude the changes of amplitude and phase of image content, which are introduced by the loss of code bits. As Fig. 11 illustrate, (a) gives the scatter plot of distribution of objective and subjective scores, and (b)–(d) show the normalized histogram of CC, RMSE and ROCC. The specific statistical values are presented in Table 4.

Table 4
The comparison of two algorithms on FF.

	CC	RMSE	ROCC
Ref. [9]			
Mean	0.7212	19.2991	0.7126
St. D.	0.0745	1.9953	0.0567
Proposed			
Mean	0.8527	14.6737	0.8231
St. D.	0.0389	1.8390	0.0450

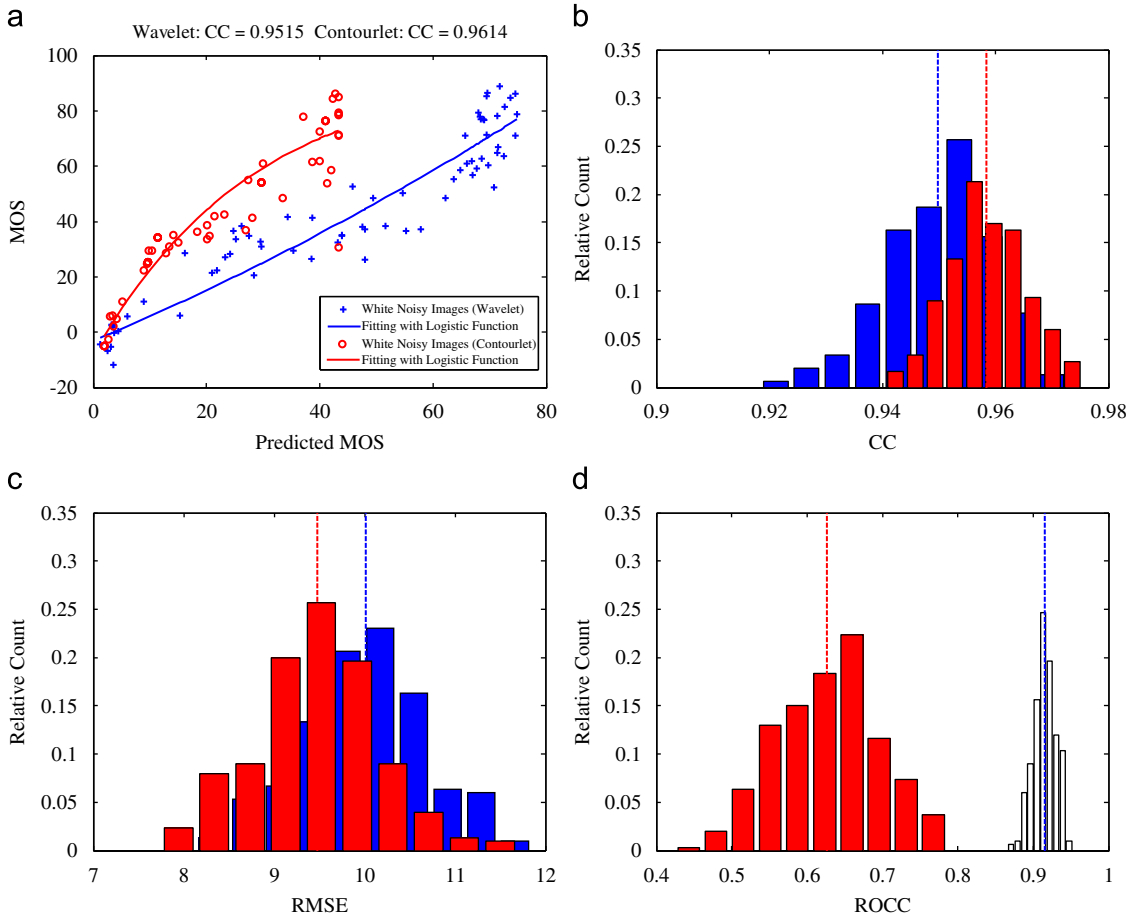

Fig. 12. The comparison of the proposed and [9] on WN.

Table 5
The comparison of two algorithms on WN.

	CC	RMSE	ROCC
Ref. [9]			
Mean	0.9498	10.0595	0.9151
St. D.	0.0094	0.6615	0.0145
Proposed			
Mean	0.9576	9.5970	0.6005
St. D.	0.0070	0.7421	0.0690

From Figs. 11, we can see that the proposed method could measure the FF image quality by quantizing the loss of high frequency proponents. It achieves correlations of around 0.8527 with subjective scores on the test sets, which is quite a good prediction performance for NR metric.

3.3.5. *Results of WN images*

WN images are contaminated by simply adding original image with different grades of white noise. Because white noisy images lost their low frequency proponent in distortion, the image quality can be calculated by low frequency. The comparison can be seen from Fig. 12. The statistical data are presented in Table 5.

It is apparent from Figs. 12 that the proposed can predict image quality for different distortions that is agreed with human consumption. As a comparison, our algorithm outperforms the existing NR methods, e.g., [9,24]. Although the proposed is not comparable to the state-of-art of reference IQA methods, it provides an available solution for NR IQA problem. The precise modeling of image can be an effective way to measure image degradations.

4. Conclusion

In this paper, an improved image model is proposed to do image quality assessment without any reference by capturing the image structural information. The image is decomposed by contourlet into multiscale and multidirectional subbands. The nonlinear dependencies are captured by the joint histograms of the reference and estimated contourlet coefficients. An image-dependent threshold is employed to eliminate the influence of content. The final objective quality score is calculated by the nonlinear combination of the extracted features. Although the proposed is well consistent with the human perception, there are still advanced approaches of the image model [25] deserve to further investigate for IQA in the future.

Acknowledgements

We thank constructive suggestions from anonymous reviewers. This research was supported by National Science Foundation of China (60771068, 60702061, 60832005), the Open-End Fund of National Laboratory of Pattern Recognition in China and National Laboratory of Automatic Target Recognition, Shenzhen University, China, the Program for Changjiang Scholars and innovative Research Team in University of China (IRT0645), the Nanyang Technological University Nanyang SUG Grant (under project number M58020010), the Microsoft Operations PTE LTD–NTU Joint R&D (M48020065), and the K. C. Wong Education Foundation Award.

References

[1] Methodology for the subjective assessment of the quality of television pictures, Recommendation ITU-R Rec. BT. 500–11.
[2] Z. Liu, S. Sarkar, Effect of silhouette quality on hard problems in gait recognition, IEEE Transactions on Systems, Man, and Cybernetics—Part B: Cybernetics 35 (2) (2005) 170–183.
[3] Z. Wang, A.C. Bovik, Modern Image Quality Assessment, Morgan and Claypool Publishing Company, New York, 2006.
[4] K. Choi, H. Choi, S. Lee, J. Kim, Fingerprint image mosaicking by recursive ridge mapping, IEEE Transactions on Systems, Man, and Cybernetics—Part B: Cybernetics 37 (5) (2007) 1191–1203.
[5] N.G. Bourbakis, Emulating human visual perception for measuring difference in images using an SPN graph approach, IEEE Transactions on Systems, Man, and Cybernetics—Part B: Cybernetics 32 (2) (2002) 191–201.
[6] H.R. Sheikh, M.F. Sabir, A.C. Bovik, A statistical evaluation of recent full reference image quality assessment algorithms, IEEE Transactions on Image Processing 15 (11) (2006) 3440–3451.
[7] K.A. Panetta, E.J. Wharton, S.S. Agaian, Human visual system-based image enhancement and logarithmic contrast measure, IEEE Transactions on Systems, Man, and Cybernetics—Part B: Cybernetics 38 (1) (2008) 174–188.
[8] Z. Wang, G. Wu, H.R. Sheikh, E.P. Simoncelli, E.-H. Yang, A.C. Bovik, Quality-aware images, IEEE Transactions on Image Processing 15 (6) (2006) 1680–1689.
[9] H.R. Sheikh, A.C. Bovik, L. Cormack, No-reference quality assessment using natural scene statistics: JPEG2000, IEEE Transactions on Image Processing 14 (11) (2005) 1918–1927.
[10] Z. Wang, A.C. Bovik, H.R. Sheikh, E.P. Simoncelli, Image quality assessment: from error visibility to structural similarity, IEEE Transactions on Image Processing 13 (4) (2004) 600–612.
[11] H.R. Sheikh, A.C. Bovik, G. de Veciana, An information fidelity criterion for image quality assessment using natural scene statistics, IEEE Transactions on Image Processing 14 (12) (2005) 2117–2128.
[12] Z. Wang, H.R. Sheikh, A.C. Bovik, No-reference perceptual quality assessment of JPEG compressed images, in: Proceedings of the IEEE International Conference on Image Processing, vol. 1, 2002, pp. I-477–I-480.
[13] A.C. Bovik, S. Liu, DCT-domain blind measurement of blocking artifacts in DCT-coded images, in Proceedings of the IEEE International Conference on Acoustic, Speech, and Signal Processing, vol. 3, 2001, pp. 1725–1728.
[14] T. Mei, X.-S. Hua, C.-Z. Zhu, H.-Q. Zhou, S. Li, Home video visual quality assessment with spatio-temporal factors, IEEE Transactions on Circuits and Systems for Video Technology 17 (6) (2007) 699–706.
[15] Y. Luo, X. Tang, Photo and video quality evaluation: focusing on the subject, in: ECCV 2008, Part III, LNCS 5304, 2008, pp. 386–399.
[16] B.R. Venkatesh, A. Perkis, An HVS-based no-reference perceptual quality assessment of JPEG coded images using neural networks, in: Proceedings of the IEEE International Conference on Image Processing, vol. 1, 2005, pp. I-433–I-436.
[17] S. Mallat, A theory for multiresolution signal decomposition: the wavelet representation, IEEE Transactions on Pattern Analysis and Machine Intelligence 11 (7) (1989) 674–693.
[18] E.P. Simoncelli, Modeling the joint statistics of images in the wavelet domain, in: Proceedings of the SPIE 44th Annual Meeting, pp. 188–195, 1999.
[19] R.W. Buccigrossi, E.P. Simoncelli, Image compression via joint statistical characterization in the wavelet domain, IEEE Transactions on Image Processing 8 (12) (1999) 1688–1701.
[20] M.N. Do, M. Vetterli, The contourlet transform: an efficient directional multiresolution image representation, IEEE Transactions on Image Processing 14 (12) (2005) 2091–2106.
[21] D.D.-Y. Po, M.N. Do, Directional multiscale modeling of images using the contourlet transform, IEEE Transactions on Image Processing 15 (6) (2006) 1610–1620.
[22] H.R. Sheikh, Z. Wang, L. Cormack, A.C. Bovik, LIVE Image Quality Assessment Database, 2003, available online: 〈http://live.ece.utexas.edu/research/quality〉.
[23] Final Report from the Video Quality Experts Group on the Validation of Objective Models of Video Quality Assessment, 2000. VQEG, available online: 〈http://www.vqeg.org/〉.
[24] P. Marziliano, F. Dufaux, S. Winkler, T. Ebrahimi, Perceptual blur and ringing metrics: application to JPEG2000, Signal Processing: Image Communication 19 (2) (2004) 163–172.
[25] E.P. Simoncelli, Statistical modeling of photographic images, in: A.C. Bovik (Ed.), Handbook of Image and Video Processing, second ed., Academic Press, NY, 2005, pp. 431–441.
[26] D. Tao, X. Li, W. Lu, X. Gao, Reduced-reference IQA in contourlet domain, IEEE Transactions on Systems, Man and Cybernetics, Part B: Cybernetics 39 (6) (2009) 1623–1627.
[27] X. Gao, W. Lu, D. Tao, X. Li, Image quality assessment based on multiscale geometric analysis, IEEE Transactions on Image Processing 18 (7) (2009) 1608–1622.
[28] W. Lu, X. Gao, D. Tao, X. Li, A Wavelet-based image quality assessment method, International Journal of Wavelets, Multiresolution and Information Processing 6 (4) (2008) 541–551.
[29] W. Lu, X. Gao, X. Li, D. Tao, An image quality assessment metric based on contourlet, IEEE International Conference on Image Processing (2008) 1172–1175.

Wen Lu received his B.Eng. degree from the Xidian University in 2002, his M.Phil. degrees from the Xidian University in 2006, his Ph.D. degree in Pattern Recognition & Intelligent System at the Xidian University in 2009. Currently, he is a lecturer with the School of Electrical Engineering in the Xidian University.

His research interests include image & video understand, visual quality assessment, and computational vision. He has published a book and around 20 scientific papers including IEEE TIP, TSMC, etc. E-mail: terry.luwen@gmail.com

Kai Zeng received his B.S. degree in Electrical Engineering from the Xidian University in 2006, and his M.S. degrees from the Xidian University in 2009. He is currently pursuing his Ph.D. degree in University of Waterloo, Canada. His research interests include image & video quality assessment. E-mail: zengkai045@gmail.com

Dacheng Tao received the B.Eng. degree from the University of Science and Technology of China (USTC), the M.Phil degree from the Chinese University of Hong Kong (CUHK), and the Ph.D. degree from the University of London (Lon). Currently, he is a Nanyang Assistant Professor with the School of Computer Engineering in the Nanyang Technological University and a Visiting Research Fellow in Lon. He is a Visiting Professor in the Xi Dian University and a Guest Professor in the Wu Han University.

His research is mainly on applying statistics and mathematics for data analysis problems in data mining, computer vision, machine learning, multimedia, and visual surveillance. He has published around 100 scientific papers including IEEE TPAMI, TKDE, TIP, CVPR, ECCV, ICDM; ACM TKDD, Multimedia, KDD, etc., with best paper runner up awards and finalists. One of his TPAMI papers received an interview with ScienceWatch.com (Thomson Scientific). His H-Index in google scholar is 12 and his Erdös number is 3. Previously he gained several Meritorious Awards from the International Interdisciplinary Contest in Modeling, which is the highest level mathematical modeling contest in the world, organized by COMAP.

He is an associate editor of IEEE Transactions on Knowledge and Data Engineering, Neurocomputing (Elsevier) and the Official Journal of the International Association for Statistical Computing—Computational Statistics & Data Analysis (Elsevier). He is an editorial board member of Advances in Multimedia (Hindawi). He has authored/edited six books and eight journal special issues. He has (co-)chaired for special sessions, invited sessions, workshops, panels and conferences. He has served with more than 80 major international conferences including CVPR, ICCV, ECCV, ICDM, KDD, and Multimedia, and more than 30 prestigious international journals including TPAMI, TKDE, TOIS, and TIP. He is a member of IEEE, IEEE Computer Society, IEEE Signal Processing Society, IEEE SMC Society, and IEEE SMC Technical Committee on Cognitive Computing.

Yuan Yuan is currently a lecturer with the School of Engineering and Applied Science, Aston University, United Kingdom. She received her B.Eng. degree from the University of Science and Technology of China, China, and her Ph.D. degree from the University of Bath, United Kingdom. She has over 60 scientific publications in journals and conferences on visual information processing, compression, retrieval, etc. She is an associate editor of International Journal of Image and Graphics (World Scientific), an editorial board member of Journal of Multimedia (Academy Publisher), a guest editor of Signal Processing (Elsevier), and a guest editor of Recent Patents on Electrical Engineering. She was a chair of some conference sessions, and a member of program committees of many conferences. She is a reviewer for several IEEE transactions, other international journals and conferences. E-Mail: yuany1@aston.ac.uk

Xinbo Gao received his B.Sc., M.Sc. and Ph.D. degrees in Signal and Information Processing from the Xidian University, China, in 1994, 1997 and 1999, respectively. From 1997 to 1998, he was a research fellow in the Department of Computer Science at the Shizuoka University, Japan. From 2000 to 2001, he was a postdoctoral research fellow in the Department of Information Engineering at the Chinese University of Hong Kong. Since 2001, he joined the School of Electronic Engineering at the Xidian University. Currently, he is a Professor of Pattern Recognition and Intelligent System, and Director of the VIPS Lab, Xidian University. His research interests are computational intelligence, machine learning, computer vision, pattern recognition and artificial intelligence. In these areas, he has published 4 books and around 100 technical articles in refereed journals and proceedings including IEEE TIP, TCSVT, TNN, TSMC, etc. He is on the editorial boards of journals including EURASIP Signal Processing and Neurocomputing (Elsevier). He served as general chair/co-chair or program committee chair/co-chair or PC member for around 30 major international conferences. Email: xbgao.xidian@gmail.com